

# Spatial and temporal changes in phosphorus partitioning within a freshwater cyanobacterial mat community

Jakub Borovec · Dagmara Sirová · Petra Mošnerová ·  
Eliška Rejmánková · Jaroslav Vrba

Received: 30 October 2009 / Accepted: 2 June 2010 / Published online: 17 June 2010  
© Springer Science+Business Media B.V. 2010

**Abstract** Spatial and temporal changes in phosphorus (P) distribution, partitioning and mobility in the benthic cyanobacterial mat (CBM) were evaluated using sequential chemical fractionation. Total P (TP) content was extremely low, ranging from 0.025 to 0.1 mg g<sup>-1</sup> DW. Exchangeable and loosely bound P, which we consider to be mainly associated with extracellular polymeric substances (EPS), constituted the most significant proportion of TP (up to 52%, 55 µg g<sup>-1</sup> DW), followed by P associated with the authigenic apatites (up to 35% of TP or 18 µg g<sup>-1</sup> DW). While we found virtually no exchange of P with the ambient environment, our results show that the partitioning of P forms within

CBM is dependent on spatial and temporal fluctuations of physico-chemical parameters, mainly pH and dissolved oxygen. A conspicuous diurnal increase in the reactive, exchangeable and loosely bound P in the top CBM layers was observed. This observation has important ecological implications, as CBM microorganisms therefore have an increased possibility for P “luxury” uptake during the night. This hypothesis is further supported by the fact that P in the organic fraction rises by as much as 53% in the upper layers during the night, indicating some form of cellular uptake. The P-binding potential of EPS also has ecological or biogeochemical consequences and should be considered in stoichiometrical studies where it represents potential danger for great overestimates of cellular P values or the nutritional status of cells.

**Keywords** Phosphorus partitioning · Diurnal changes · Sequential fractionation · Cyanobacterial mat · EPS

---

J. Borovec · D. Sirová (✉) · P. Mošnerová · J. Vrba  
Institute of Hydrobiology, Biology Centre AS CR,  
Na Sádkách 7, 37005 České Budějovice, Czech Republic  
e-mail: dagmara\_sirova@hotmail.com

J. Borovec · D. Sirová · P. Mošnerová · J. Vrba  
Department of Ecosystem Biology, University of South  
Bohemia, Faculty of Science, Branišovská 31,  
37005 České Budějovice, Czech Republic

E. Rejmánková  
Department of Environmental Science and Policy,  
University of California Davis, One Shields Avenue,  
Davis, CA 95616, USA

## Introduction

Microbial mats are taxonomically complex, metabolically interactive, self-sustaining communities. They are frequently found in environments where extreme conditions in temperature, hydrology, salinity, or nutrient availability place constraints on the

occurrence of grazing invertebrates (Jørgensen et al. 1983). Often a number of phototrophic and heterotrophic microbial assemblages occur vertically stratified in microbial mats due to extreme environmental (light, oxygen, redox, pH, etc.) fluctuations on a microscopic scale (Stal 1995). Resident microorganisms release a variety of high-molecular-weight extracellular polymeric substances (EPS) and the resulting EPS matrix regulates the diffusion, binding and storage of ions and nutrients, reduces desiccation, enhances the cohesiveness and physical stability of the mat, provides microspatial organization for microbial cells (Decho 1999), and provides a template for the biogenic calcium carbonate precipitation (Braissant et al. 2009).

As the majority of microorganisms in nature persist in cooperative consortia or biofilms (Moons et al. 2009), microbial mats are viewed as important model systems for studies of ecological relationships (Stal and Caumette 1994) and studies on mat biogeochemical cycles have significantly advanced our knowledge of microbial ecology (Paerl et al. 2000). Although the biogeochemistry of carbon (C), nitrogen (N), oxygen, and sulphur within microbial mats has been extensively researched (for review see Des Marais 1995), the information regarding the cycling of phosphorus (P), its availability, partitioning, and role it plays in shaping microbial consortia within microbial mats is largely missing. Phosphorus is an essential element for all living organisms, it is involved in most cellular processes, and its supply in aquatic ecosystems is generally low (Vadstein 2000). As an essential and often limiting macronutrient, P is subject to intense biological cycling such that reactions of P compounds in aquatic environments are dominated by biota and catalyzed by the enzymes they produce (Blake et al. 2005).

We have chosen benthic microbial mats from a shallow freshwater marsh in northern Belize as a model system for studying processes related to P cycling within complex consortia. The study location is a part of phytogeographically related, limestone-based marshes covering extensive areas of the Caribbean, mainly Yucatan peninsula and southern Florida (Rejmánková et al. 1996). These herbaceous wetland ecosystems are characterized by extreme P limitation, resulting in low diversity and sparse growth of macrophytes as well as invertebrate

grazers. The reduced competition from higher plants and reduced grazing pressure favour the development of thick benthic microbial mats, dominated by cyanobacteria. The cyanobacterial mats (CBM) constitute a major part of biomass and primary production, coupled with relatively high rates of nitrogen fixation (Rejmánková and Komárková 2000). They also significantly influence sediment formation contributing biogenic calcium carbonate to the extensive marl deposits characteristic for the area (Kim and Rejmánková 2002). Regardless of the strong nutrient limitation, the species richness of cyanobacteria was found to be unusually high (Rejmánková et al. 2004; Komárek and Komárková-Legnerová 2007).

Results from previous studies indicate that P-limitation is an important driving force in Caribbean CBM. According to Gaiser et al. (2004), P in periphyton mats provides the best metric for detecting low-level P enrichment in oligotrophic wetlands, which is consistent with the rapid uptake of labile P from the water column by both biotic and abiotic components of the CBM detected in radioisotope tracing studies (Scinto and Reddy 2003; Noe et al. 2003). High extracellular alkaline phosphatase activity, located mainly in the EPS matrix, was found within the CBM (Sharma et al. 2005; Sirová et al. 2006). This large pool of free dissolved phosphatase was hypothesized to improve the flux of limited P supplies into the mat matrix by enhancing hydrolysis of organic P compounds (Sirová et al. 2006). Experimental P addition resulted in a significant increase in primary production and N<sub>2</sub> fixation of CBM, while it suppressed the activity of extracellular alkaline phosphatase and decreased cyanobacterial diversity and CBM structural integrity (Rejmánková and Komárková 2000, 2005; Richardson et al. 2008).

There are many questions regarding P cycling in CBM that cannot be answered without first gaining the understanding of P distribution and how its partitioning is influenced by the physico-chemical parameters. The aim of this work is to provide information on changes in P distribution, availability, and mobility in the pore water and between various chemical fractions of CBM particulate matter, both in the vertical profile and diurnally. We hope these results will aid in future research of the biogeochemistry of complex microbial communities.

## Materials and methods

### Study site and cyanobacterial mats

The selected location is included in long term research of Belizean wetland ecology and its environmental characteristics have been published previously (Sirová et al. 2006). The studied marsh covers 11.3 ha, with marl-dominated sediment and the following water column chemistry: pH 7.8; conductivity  $143 \mu\text{S cm}^{-1}$ ; alkalinity  $1143 \text{ meq L}^{-1}$ ; soluble reactive phosphorus (SRP)  $2.9 \mu\text{g L}^{-1}$ ; TP  $5.5 \mu\text{g L}^{-1}$ ;  $\text{NH}_4\text{-N}$   $6.0 \mu\text{g L}^{-1}$ ;  $\text{NO}_3\text{-N}$  below detection limit,  $\text{NO}_2\text{-N}$   $2 \mu\text{g L}^{-1}$ ;  $\text{SO}_4^{2-}$   $1.0 \text{ mg L}^{-1}$ ;  $\text{Cl}^-$   $8.3 \text{ mg L}^{-1}$ ; and  $\text{Ca}^{2+}$   $16.5 \text{ mg L}^{-1}$ .

Cyanobacterial mats at the study location have a cohesive, cotton-wool-like texture, range from 3 to 10 cm in thickness and undergo seasonal development cycle which is dependent on rainfall patterns (Rejmánková and Komárková 2000). Mat surface is smooth, with protruding cyanobacterial filaments and mats typically follow the relief of the underlying sediment. Filamentous non-heterocystous cyanobacteria of the genus *Leptolyngbya* constitute most of the mat biomass, with many other filamentous and unicellular species intermingled. *Microcoleus chthonoplastes*, a cyanobacterium commonly found to dominate many of the cyanobacterial mats studied elsewhere, is entirely absent in these systems (Rejmánková et al. 2004). The mat biomass ranges from 200 to  $700 \text{ g AFDM m}^{-2}$  (Rejmánková and Komárková 2000).

### In situ microsensor measurements and sample collection

In January 2007, diurnal in situ microsensor profiles of dissolved oxygen (DO) and pH were measured using microelectrodes (Unisense, Denmark) connected to a data logger (Fiedler-Mágr, Czech Rep.). Microsensors were fixed in a battery-driven motorized micromanipulator connected to a heavy stand, with signal collection selected at 1 mm depth interval. The depth of water column at the time of data collection was 60 cm; water temperature fluctuated between 25–26°C.

After completing microsensor measurements, eight cores (7 cm in diameter) which included CBM and 4 cm of the underlying sediment were collected from the immediate vicinity, at 5:00 pm (“day” cores) and

5:00 am (“night” cores), when the largest differences in measured parameters were observed. Cores were frozen immediately, dissected into 12 layers 4 mm thick representing individual samples, and stored at  $-18^\circ\text{C}$  until further analysis.

### Cyanobacterial mat sample processing

Each sample was gently homogenized by a hand-held 15 mL Dounce homogenizer. This procedure (1 stroke) disrupted CBM structure without significant cell damage. A small sub-sample was used to determine the dry mass (DM), loss on ignition (LoI), and total contents of carbon (TC), inorganic carbon (TIC), nitrogen (TN), phosphorus (TP), iron (Fe), and calcium (Ca). The remainder was centrifuged (1100 g, 20 min) and pore water (PW) removed for chemical analyses. Soluble reactive phosphorus (SRP) and total dissolved P (TDP) were determined in PW sample after its filtration ( $0.4 \mu\text{m}$ , MN GF-5, Macherey Nagel, Germany).

### Phosphorus fractionation

Following PW removal, the pellet was subjected to a sequential P fractionation according to Ruttenberg (1992; later modified by Jensen et al. 1998) to determine P composition in the vertical CBM profile. The successive fractionation steps along with extracted P forms are described in Table 1. Known amount of sample (approximately 0.1 g DW) was extracted by 15 mL of extractant. Each extraction step was terminated by a short wash (5 mL) by the extractant.

This methodology has been developed specifically for carbonate rich sediments or soils which mainly consist of mineral particles. The interpretation of successive extraction steps in the case of predominantly organic CBM therefore needed to be verified. We have conducted a series of laboratory experiments on pure cultures of cyanobacteria, algae and bacteria (data not shown), and established that P associated with the 0.1 M NaOH was mostly non-reactive, cellular in origin. In the case of slime-producing organisms (the cyanobacterium *Chroococcus* sp.), significant amounts of SRP were found in the first (1 M  $\text{MgCl}_2$ ) fraction, which was regarded as EPS-bound (cf. Klock et al. 2007). In order to verify that microbial EPS was indeed extracted by the first

**Table 1** Successive steps of P fractionation

Step/Fraction	Extraction (time/temperature)	P-forms	
1. MgCl <sub>2</sub>	1 M MgCl <sub>2</sub> (1 h/25°C) + rinse, pH 8.0	SRP	Dissolved and loosely bound inorganic P (including EPS)
		NRP	Dissolved and loosely bound organic P (including EPS)
2. BD	0.1 M Na <sub>2</sub> S <sub>2</sub> O <sub>4</sub> + 0.1 M NaHCO <sub>3</sub> (1 h/25°C) + rinse, pH 7.2	SRP	Redox-sensitive P bound to Fe (Mn) hydroxides and compounds
		NRP	P-bound to organic matter sorbed on Fe hydroxides
3. NaOH	0.1 M NaOH (16 h/25°C) + rinse	SRP	P bound to metal (Al) oxy-hydroxides, some low-molecular weight phosphorylated molecules
		NRP	P bound in precipitates of humic compounds with metals; P in living microbial cells including poly-P and cellular remains
4. Na-Ac	1 M Na-Ac (4 h/25°C) + rinse, pH 4.0	SRP	P bound to freshly precipitated carbonates and apatites
		NRP	Acid labile organic P
5. HCl	0.5 M HCl (24 h/25°C) + rinse	SRP	P bound to residual carbonates
		NRP	Acid labile organic P
6. NaOH <sub>85</sub>	1 M NaOH (24 h/85°C) + rinse	SRP	Refractory and other organic P
		NRP	

BD bicarbonate dithionate, SRP soluble reactive P, NRP non-reactive P, NRP = TDP – SRP

reagent in this fraction, we determined total carbohydrate content according to Dubois et al. (1956).

#### Quantification of CBM nutrient pools

To determine whether CBM exchange C, N, and P with the water column and internal shifts in P pools during the diurnal cycle, we calculated the amount of each of the nutrients in the entire core as a sum of their masses in the 12 layers (mass per layer = the concentration of each nutrient in a layer × DM in a layer × layer volume).

#### Analytical methods

Dry mass was determined gravimetrically by the drying of samples at 105°C to constant weight, LoI by ashing at 550°C for 2 h. TC, TIC, and TN concentrations were determined using NC 2100 Soil Analyzer (ThermoQuest, Italy), TDP, TP, and Fe concentrations were measured by colorimetry after nitric-perchloric acid digestion (Kopáček et al. 2001) using Flow Injection Analyzer (QuickChem 8500, Lachat, USA). Soluble reactive phosphorus concentrations were determined by colorimetry (Murphy and Riley 1962). The detection limit for P analyses used in our laboratory is 1 µg L<sup>-1</sup> P. The colorimetric determination of P concentration was repeated twice

for verification and values displayed are therefore a mean of two measurements. More detail on the methodology can be found in Kopáček et al. 2001. The calcium concentrations were determined by AAS (Varian, USA) in perchloric digests.

## Results

### Diurnal dynamics of DO and pH

For better clarity, we have divided the CBM vertical profile into three optically distinguishable zones with different physico-chemical characteristics: top “yellow”, middle “green”, and bottom “red” layers, termed according to the colour caused by dominant cyanobacterial or bacterial pigments (scytonemin, chlorophyll, and bacterial carotenoids, respectively).

The DO concentration and pH in the mat underwent large diurnal and vertical fluctuations (Fig. 1a), except for the bottom-most red layer, which experienced permanent anoxia and pH of around 7.5 (Fig. 1b). During the day, the top 7 mm of the mat were supersaturated by oxygen with the highest measured pH values above 9. The entire mat profile turned anoxic approximately an hour before sunrise.

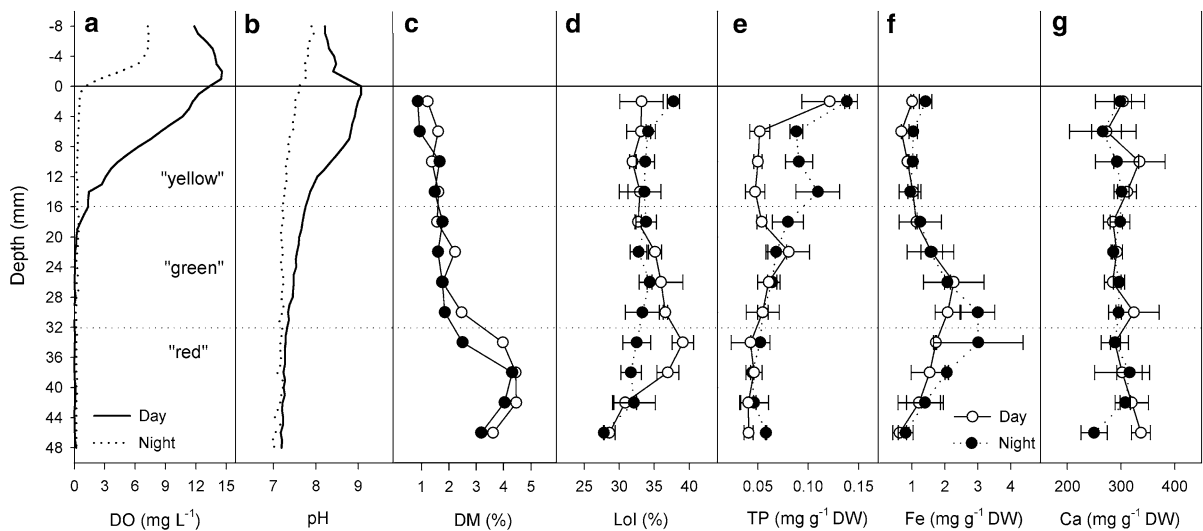


**Fig. 1** Diurnal changes in selected physico-chemical parameters of studied CBM at 5:00 pm (day) and 5:00 am (night). **a** dissolved oxygen (DO) profiles, **b** pH profiles, **c** dry mass (DM), **d** loss on ignition (LoI), **e** total phosphorus (TP), **f** Fe

total content, **g** Ca total content. Data points in **d**, **e**, **f**, **g** represent averages ( $\pm$ SD,  $n = 3$ ). Horizontal dotted lines separate the top yellow, middle green and bottom red CBM layers defined for experimental purposes

### General characteristics of the CBM cores

Low DM ranging  $1.4 \pm 0.3\%$  in the yellow layer to  $3.9 \pm 0.7\%$  in the red (Fig. 1c), together with LoI values between 30–40% (Fig. 1d), indicated high pore water content and a large proportion of organic matter in particles. Pore water TDP represented only 4% of the CBM TP during both day and night. The SRP (Fig. 2c) which constituted 50–75% of pore water TDP, however, rose significantly (layers from 0 to 24 mm;  $P < 0.05$ ,  $df = 2$ ) in the yellow and green layers during the night (Fig. 2c).

Total C (TC) content was 220–240  $\text{mg g}^{-1}$  DW, 32–38% of which was carbonate C. The highest TC and carbonate content was found in the top-most few mm of the mat. Total P content was extremely low, ranging from 0.025 to 0.1  $\text{mg g}^{-1}$  DW, with a significant increase (layers from 4 to 20 mm;  $P < 0.05$ ,  $df = 2$ ) in the yellow layer during the night (Fig. 1e). Iron and Ca remained approximately constant diurnally in the entire profile of the mat, except for the notable but statistically insignificant rise in the night-time Fe concentration in the transition zone between the green and red layer (Fig. 1f, g).

### Phosphorus fractionation of CBM particulate matter and diurnal changes in P partitioning

The three optically distinguishable layers corresponded well with diurnal partitioning of P forms in the CBM vertical profile. Overall, most of the P found in the CBM solid particles was found in the exchangeable and loosely bound and authigenic apatite associated fraction (Table 2, Fig. 2). The possible analytical error of each fractionation result is between 5–10%, however only P concentration changes larger than 30% were considered as important while evaluating the results below.

#### Exchangeable and loosely bound P

Exchangeable and loosely bound P (1 M  $\text{MgCl}_2$ ) constituted the largest proportion of P pool in the yellow layer during both day and night (28% and 52% of TDP, respectively) and the green layer during the day (30% of TDP). This fraction also exhibited largest diurnal changes: day TDP concentration ( $14 \mu\text{g g}^{-1}$  DW) increased more than twice ( $40 \mu\text{g g}^{-1}$  DW) in the yellow layer, contrary to the marked night-time concentration decrease in the green layer (from 16 to  $5 \mu\text{g g}^{-1}$  DW, see Fig. 2).

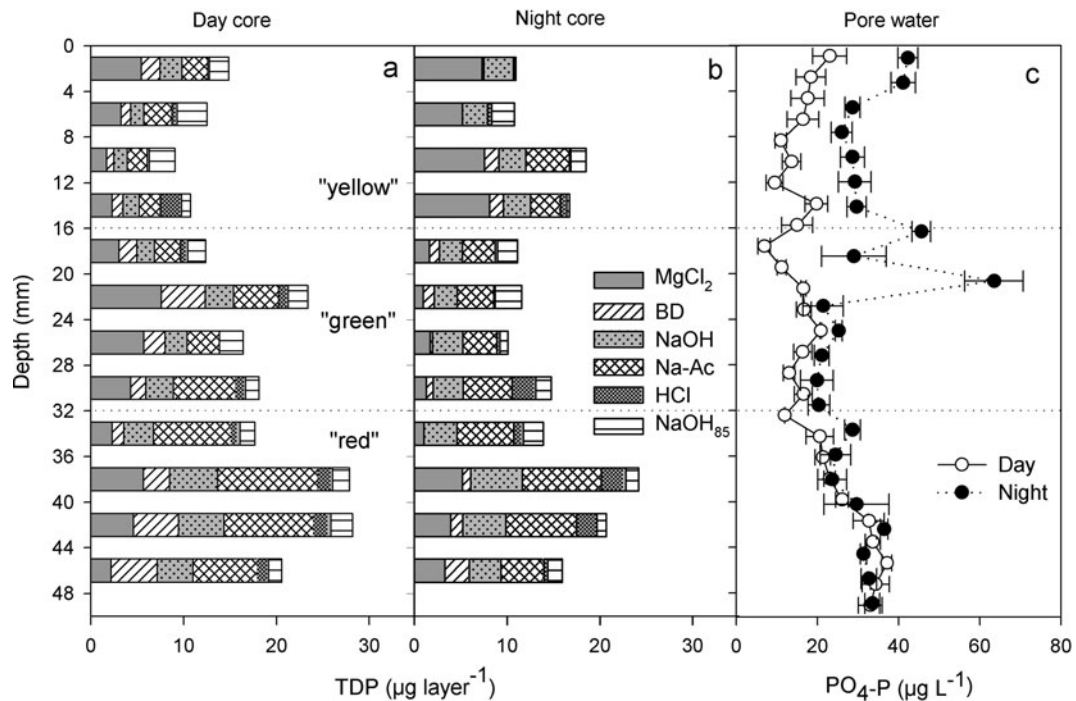


**Fig. 2** Total dissolved phosphorus (TDP) content in the sequential chemical fractions analyzed in the day (a) and night (b), and diurnal changes in pore water concentrations ( $\pm$  SD,  $n = 3$ ) of soluble reactive P (SRP) (c). (BD—bicarbonate

dithionate). Horizontal dotted lines separate the top yellow, middle green and bottom red CBM layers defined for experimental purposes

**Table 2** Summary of P fractionation results (TDP/SRP, in  $\mu\text{g g}^{-1}$  DW) for the day and night cores in particular CBM layers (depth in mm). Averages for the yellow, green and red layers are shown at the bottom of the table. (BD – bicarbonate dithionate)

Layer	Depth	Day core (fractions)						Night core (fractions)					
		MgCl <sub>2</sub>	BD	NaOH	Na-Ac	HCl	NaOH <sub>85</sub>	MgCl <sub>2</sub>	BD	NaOH	Na-Ac	HCl	NaOH <sub>85</sub>
Yellow	0–4	28/17	10/8	12/0	14/4	1/0	10/1	55/54	1/1	24/11	0/0	1/0	1/1
	4–8	13/11	4/4	5/0	12/7	2/0	13/5	36/34	0/0	19/8	0/0	3/0	17/5
	8–12	8/5	4/3	6/1	10/6	1/0	13/0	30/16	6/6	11/6	18/12	1/0	6/2
	12–16	9/5	5/1	7/0	9/7	9/0	4/0	36/17	7/6	13/6	14/12	3/0	2/1
Green	16–20	12/8	8/5	7/1	11/11	3/0	8/1	6/4	4/3	9/3	13/12	1/0	8/2
	20–24	21/21	13/10	9/2	14/9	3/0	6/0	4/1	5/3	10/5	16/13	1/0	12/2
	24–28	20/5	8/5	8/2	12/11	0/0	9/1	6/0	1/0	12/5	14/13	1/0	3/3
	28–32	11/2	5/4	8/0	17/12	3/1	4/1	5/1	3/3	11/4	18/14	9/3	6/6
Red	32–36	4/1	2/1	5/1	13/11	1/1	3/1	3/0	0/0	9/3	16/14	3/1	6/4
	36–40	8/3	4/3	7/2	15/11	3/2	8/5	8/1	1/2	8/4	13/13	4/1	2/5
	40–44	6/3	7/5	7/2	14/11	3/1	10/1	6/3	2/3	7/4	12/12	4/1	2/5
	44–48	4/3	9/7	7/2	12/9	2/1	7/2	7/3	5/2	7/3	9/9	1/0	4/3
Average	Yellow	14/10	6/4	8/0	11/6	3/0	10/1	39/30	4/3	17/8	8/6	2/0	6/2
	Green	16/9	8/5	8/1	14/11	2/0	7/1	5/2	3/2	11/4	15/13	3/1	7/3
	Red	6/2	5/4	7/2	14/11	2/2	7/2	6/2	2/2	8/4	13/12	3/1	3/5

Similarly, diurnal changes affected the composition of  $\text{MgCl}_2$  fraction: The SRP concentration increased from 72 to 90% of TDP in this fraction during the night in the yellow layer, while a marked decrease from 96 to 30% was observed in the green layer.

Exchangeable and loosely bound P was not a dominant P form in the red layer, where it constituted only 14 and 17% of TDP during the day and night.

#### Phosphorus associated with authigenic apatites

In the red layer, this form of P constituted the majority of TP during both day and night (approximately 35%). It was also the second most important fraction in the yellow and green layer during the day, amounting to approximately a quarter of TP (Table 2). A marked decrease in authigenic apatite associated P concentration in the yellow and slight increase in the green layer was observed during the night. Soluble reactive P concentration in this fraction was also subject to diurnal changes, increasing in all layers, most notably the yellow layer (from 73 to 98% of TP) during the night (Table 2).

#### Other P fractions

Although the mats were found to be low in Fe content (0.64–2.28  $\text{mg g}^{-1}$  DW, see Fig. 1), the concentration of redox-labile (Fe-bound) P was not negligible (11–15% of TDP during the day and 5–7% of TDP during the night, see Table 2).

Total organically bound P (0.1 M NaOH) was uniformly distributed across all three layers, rising by 27% in the green layer and by as much as 53% in the red layer during the night. This night-time increase constituted almost entirely of SRP (Table 2).

Phosphorus associated with detrital apatites (HCl fraction) amounted to less than 10% of TDP in all layers (Table 2, Fig. 2).

The residual P showed large variation (9–19% of TDP) both vertically and diurnally, probably due to the irregular “patchy” distribution of recalcitrant organic matter in CBM (Table 2, Fig. 2).

#### Quantification of diurnal changes in CBM nutrient pools

The quantification of diurnal changes in CBM revealed marked decrease in TC and TN concentrations in the

night core compared to the day samples (18 and 17%, respectively). Changes in TP concentration, however, were negligible (a 4% rise in the night core), suggesting low exchange of P with the ambient environment.

A more detailed calculation included the PW TDP pool and first four fractions (Table 3). Comparing the diurnal changes in P amounts in the particular mat layers and P pools ( $\delta\text{P}$ ) revealed an overall difference of 29  $\mu\text{g P}$ , which was 17% of total P included in the calculation. The largest changes were detected in the yellow and green layers such that during the night, the green layer behaved as a P source and the yellow layer as P sink. Largest proportion of P released in the green layer originated in the EPS-associated fraction (16  $\mu\text{g P}$ ) and the redox labile pool (7  $\mu\text{g P}$ ). This P amount was then recovered in the EPS-associated fraction (16  $\mu\text{g P}$ ) and microbial biomass (6  $\mu\text{g P}$ ) in the yellow layer, where an additional small amount of P was released from the redox labile (2  $\mu\text{g P}$ ) and authigenic apatite (2  $\mu\text{g P}$ ) pools. Night time P

**Table 3** Quantification of CBM P pools most affected by diurnal changes, in the three mat layers

Layer	TDP ( $\mu\text{g layer}^{-1}$ )		$\delta\text{P}^{\text{a}}$ ( $\mu\text{g layer}^{-1}$ )	sum $\delta\text{P}/\text{layer}^{\text{b}}$ ( $\mu\text{g}$ )
	Day core	Night core		
Yellow				
PW	1	2	−1	−19
MgCl <sub>2</sub>	13	29	−16	
BD	5	3	2	
NaOH	7	13	−6	
Na-Ac	10	8	2	
Green				
PW	1	2	−1	22
MgCl <sub>2</sub>	21	5	16	
BD	11	3	7	
NaOH	10	11	−1	
Na-Ac	18	16	1	
Red				
PW	2	2	0	3
MgCl <sub>2</sub>	15	13	1	
BD	14	13	1	
NaOH	17	17	0	
Na-Ac	28	27	1	

TDP total dissolved phosphorus

<sup>a</sup>  $\delta\text{P} = \text{Day (TDP)} - \text{Night (TDP)}$

<sup>b</sup> Sum  $\delta\text{P} = \text{sum of } \delta\text{TDP pools within the entire layer}$



increase in the PW accounted for approximately  $1 \mu\text{g layer}^{-1} \text{ P}$ .

## Discussion

It is clear that CBM are remarkably low in P, whose concentration falls below  $0.1 \text{ mg g}^{-1} \text{ DW}$ . Due to technical difficulties with analyzing material of such low P content and in finding representative CBM cores of equal length, we decided to fractionate one “day” core and one “night” core only, while performing analyses of DM, LoI, TP, iron and calcium content, and PW  $\text{PO}_4\text{-P}$  analyses in triplicates. Fractionation results could therefore not be verified statistically; however we believe our main conclusion that there is a conspicuous night time release of soluble and loosely bound P in the upper CBM layers is supported by a statistically significant rise in both TP and PW SRP (Fig. 1d).

Although majority of the CBM volume is made up of pore water, as much as 96% of TP is associated with particulate matter (this study). In CBM, particulate matter is made up of cyanobacterial and bacterial cells, both living and dead, embedded in the EPS matrix along with precipitated mineral crystals and various detritus (Sirová et al. 2006). It has been suggested previously that conditions in a photosynthetically active environment (high pH, high dissolved mineral content, and low  $\text{CO}_2$  partial pressure) favour the co-precipitation of P with  $\text{CaCO}_3$  or its adsorption onto  $\text{CaCO}_3$  crystals (Otsuki and Wetzel 1972), thus making P less available for biotic uptake. As the studied CBM meet all of these conditions and carbonates accounted for 32–38% of TC, we expected the Na-acetate fraction to be the most important P pool. This assumption proved correct only for the bottom-most red layer, which experienced condition of permanent anoxia, stable pH and according to microscopic analyses (Sirová, unpubl. data) contained dormant bacterial cysts and cyanobacterial resting stages.

In the rest of the CBM layers, majority of P was found in the exchangeable and loosely bound pool in the soluble reactive form. There is no universal method for the extraction of microbial EPS, due to large variation in EPS properties and composition, however the solution of concentrated salt used as an extraction medium for the exchangeable and loosely

bound pool fraction is also a commonly employed reagent for the extraction of EPS (Klock et al. 2007). Considering the fact that EPS is the matrix of CBM, it can be assumed that the most important P reservoir in CBM was associated with the EPS. We have verified this assumption by measuring the concentration of total sugars, which were almost entirely found in this first fraction (data not shown). The adsorptive properties of EPS have been well documented (for review see Sutherland 2001a, b). However the P binding capacity of EPS has only rarely been described and has not been considered ecologically. Cloete and Oosthuizen (2001) have shown that cell clusters with associated EPS in activated sludge systems contained between 57 and 59% P, while almost 30% was found in EPS alone. These values correspond well with our results, where, except for the red layer, 28–30% P was found in the exchangeable and loosely bound fraction during the day.

The steep decrease in DO and pH during the night, caused by the dominance of the respirative processes throughout the entire CBM, had profound influence on the partitioning of P between the first four fractions in the yellow and green layer.

It has been shown previously on a similar system (Richardson et al. 2008), that a shift from circum-neutral or slightly alkaline pH values to pH above 9 results in calcium carbonate precipitation at the mat surface. This supports our results, as we observed an increase in carbonate associated P (Na-Ac fraction) in the topmost 0–8 mm of the mat during the daytime, when pH values driven by photosynthesis rose above 9. Conversely, the soluble reactive P in these layers was released from the precipitates during the night following a drop in pH.

The most conspicuous, however, were the shifts in the exchangeable and loosely bound P concentrations. The EPS matrix varies in composition and may contain polymers synthesized by microbial cells, absorbed nutrients, metabolites, products of cell lysis, and detritus from the surrounding environment (Sutherland 2001a). It is thought that the majority of EPS macromolecules are polyanionic, although neutral and polycationic EPS have been described (Sutherland 2001b). The large number of charged groups and residues with various degree of protonation can interact readily with ions (Chandrasekaran et al. 1994) and make the binding capacity of EPS largely pH dependent. While the mechanism by



which P binds to EPS is unknown, it is possible that cations such as  $\text{Ca}^{2+}$  and  $\text{Mg}^{2+}$  (Watanabe et al. 2006) or the positively charged residues of amino-acids (Kawaguchi and Decho 2002) may play a role. The night time decrease in pH seemed to liberate exchangeable and loosely bound P, which moved, in the soluble reactive form, from the green to the yellow layer joining the SRP pool in the same fraction there. Thus, majority of the exchangeable and loosely bound P remaining in the green layer was non-reactive.

The redox-labile P form is adsorbed to the surface of or co-precipitates with Fe oxyhydroxides. Night-time decrease in DO and consequent lowering of the redox potential in the yellow and green layers caused the liberation of P from redox-labile Fe compounds. Liberated P most probably also entered the soluble reactive pool associated with the exchangeable and loosely bound fraction.

This has important ecological implications, as CBM microorganism therefore have an increased possibility for P “luxury” uptake during the night. This hypothesis seems to be further supported by the fact that P in the organic fraction (0.1 M NaOH) rose markedly in the most metabolically active upper yellow layer and the green layer below it (by 53 and 27% respectively), indicating cellular uptake. Prokaryotic cells store excess P as polyphosphate, probably, among other advantages, for osmotic reasons (Kornberg 1999). This storage polymer would normally be extracted in the 0.1 M NaOH fraction as non-reactive P (Hupfer et al. 1995). Most of the night time P increase in this fraction, however, was attributed to the soluble reactive form and hence could not be labelled as truly cytoplasmatic. This phenomenon could perhaps be explained by the accumulation of P in the periplasmic space of microbial cells. Cyanobacterial mats consists predominantly of Gram-negative cyanobacteria and bacteria, whose periplasmic space can account for 20–40% of cellular volume and is known to contain a large variety of phosphorylated compounds in significant amounts (Prescott et al. 1996). The organic 0.1 M NaOH fraction remained virtually unchanged in the red layer, supporting the assumption that the microbial cells found there were dormant.

The relatively large amounts of loosely bound, soluble reactive P, available for microbial uptake in the upper CBM layers, lead us to believe that CBM microorganisms studied were primarily limited by

other factors rather than purely by the scarcity of P. Furthermore, their ability to rapidly sequester P from the water column (Scinto and Reddy 2003) and eventually bury it in the sediment associated with precipitated carbonates deepens the P limitation of other ecosystem components such as macrophytes or planktonic communities.

It has been shown elsewhere, that microbial mats are generally at a steady state (Canfield and Des Marais 1994) and enough nutrients are made available by oxidative processes over 24 h to fuel primary production during the day, with a small additional external source to balance the small amount of nutrients buried within the mat. Organic material from lysed microbial cells is most probably released into the EPS (Frølund et al. 1996). Sirová et al. (2006) reported large activity of free alkaline phosphatase associated with the CBM EPS. The capacity of EPS to bind P may also play a role in preventing its co-precipitation with carbonates (Kawaguchi and Decho 2002) and this, together with EPS associated extracellular enzyme activity likely plays an important role in reducing P limitation in the system.

While our assumptions are made for the benthic CBM in a stage of maturity and established physico-chemical gradients, how the system behaves during the stages of rapid mat development following rewetting at the beginning of the rainy season (Rejmánková and Komárková 2000; Sirová et al. 2006) remains to be assessed.

Our results show that P is not a static nutrient, but that the partitioning of its forms and hence, presumably, its bioavailability is dependent on spatial and temporal fluctuation of physico-chemical parameters, mainly pH, in most of the vertical profile. Extracellular polymeric substances appear to bind significant amounts of P and facilitate the main diurnal shifts of P both in the vertical profile and between the reactive and non-reactive pools. The P-binding potential of EPS also has ecological or biogeochemical implications and should be considered in stoichiometrical studies where, as in the case of surface adsorbed P (Sañudo-Wilhelmy et al. 2004), cellular P values or the nutritional status of cells could be greatly overestimated.

**Acknowledgment** This research was supported by National Science Foundation grant NSF # 0516159 and partly by Czech grants NAZV QH81012, MSM 6007665801, AV0Z 60050516 and 60170517. We would like to thank Irenio and Russel for help with field sampling.

## References

- Blake RE, O'Neil JR, Surkov AV (2005) Biogeochemical cycling of phosphorus: Insights from oxygen isotope effects of phosphoenzymes. *Am J Sci* 305:596–620
- Braissant O, Decho AW, Przekop KM et al (2009) Characteristics and turnover of exopolymeric substances in a hypersaline microbial mat. *FEMS Microbiol Ecol* 67: 293–307
- Canfield DE, Des Marais DJ (1994) Cycling of carbon, sulphur, oxygen and nutrients in a microbial mat. In: Stal LJ, Caumette P (eds) *Microbial mats: structure, development and environmental significance*. NATO ASI series G, Ecological Sciences. Springer-Verlag, Berlin, Heidelberg
- Chandrasekaran R, Lee EJ, Thailambal VG et al (1994) Molecular architecture of a galactoglucan from *Rhizobium meliloti*. *Carbohydr Res* 261:279–295
- Cloete TE, Oosthuizen DJ (2001) The role of extracellular exopolymers in the removal of phosphorus from activated sludge. *Water Res* 35:3595–3598
- Decho AW (1999) Function of EPS. In: Wingender J, Neu TR, Flemming HC (eds) *Microbial extracellular polymeric substances: characterization, structure, and function*. Springer, Berlin, New York
- Des Marais DJ (1995) The biogeochemistry of hypersaline microbial mats. *Adv Microb Ecol* 14:251–274
- Dubois M, Gilles KA, Hamilton JK et al (1956) Colorimetric method for determination of sugars and related substances. *Anal Chem* 28:350–356
- Frølund B, Palmgren R, Keiding K et al (1996) Extraction of extracellular polymers from activated sludge using a cation exchange resin. *Water Res* 30:1749–1758
- Gaiser EE, Scinto LJ, Richards JH et al (2004) Phosphorus in periphyton mats provides the best metric for detecting low-level P enrichment in an oligotrophic wetland. *Water Res* 38:507–516
- Hupfer M, Gächter R, Rügger H (1995) Poly-P in lake sediments.  $^{31}\text{P}$  NMR spectroscopy as a tool for its identification. *Limnol Oceanogr* 40:610–617
- Jensen HS, McGlathery KJ, Marino R et al (1998) Forms and availability of sediment phosphorus in carbonate sand of Bermuda seagrass beds. *Limnol Oceanogr* 43:799–810
- Jørgensen BB, Revsbech NP, Cohen Y (1983) Photosynthesis and structure of benthic microbial mats: microelectrode and SEM studies of four cyanobacterial communities. *Limnol Oceanogr* 28:1075–1093
- Kawaguchi T, Decho AW (2002) Isolation and biochemical characterization of extracellular polymeric secretions (EPS) from modern soft marine stromatolites (Bahamas) and its inhibitory effect on  $\text{CaCO}_3$  precipitation. *Prep Biochem* 32:51–63
- Kim JG, Rejmánková E (2002) Recent history of sediment deposition in marl- and sand-based marshes of Belize, Central America. *Catena* 48:267–291
- Klock JH, Wieland A, Seifert R et al (2007) Extracellular polymeric substances (EPS) from cyanobacterial mats: characterisation and isolation method optimisation. *Mar Biol* 152:1077–1085
- Komárek J, Komárková-Legnerová J (2007) Taxonomic evaluation of the cyanobacterial microflora from alkaline marshes of northern Belize. 1. Phenotypic diversity of coccoid morphotypes. *Nova Hedwig* 84:65–111
- Kopáček J, Borovec J, Hejzlar J et al (2001) Spectrophotometric determination of iron, aluminum, and phosphorus in soil and sediment extracts after their nitric and perchloric acid digestion. *Commun Soil Sci Plant Anal* 32: 1431–1443
- Kornberg A (1999) Inorganic polyphosphate: a molecule of many functions. *Annu Rev Biochem* 68:89–125
- Moons P, Michiels CW, Aertsen A (2009) Bacterial interactions in biofilms. *Crit Rev Microbiol* 35:157–168
- Murphy J, Riley JP (1962) A modified single solution method for determination of phosphate in natural waters. *Anal Chim Act* 26:31–36
- Noe GB, Scinto LJ, Taylor J et al (2003) Phosphorus cycling and partitioning in an oligotrophic Everglades wetland ecosystem: a radioisotope tracing study. *Freshwater Biol* 48:1993–2008
- Otsuki A, Wetzel RG (1972) Coprecipitation of phosphate with carbonates in a marl lake. *Limnol Oceanogr* 17:763–767
- Paerl HW, Pinckney JL, Steppe TF (2000) Cyanobacterial-bacterial mat consortia: examining the functional unit of microbial survival and growth in extreme environments. *Environ Microbiol* 2:11–26
- Prescott LM, Harley JP, Klein DA (1996) *Microbiology*, 3rd edn. McGraw-Hill, New York, pp 51–52
- Rejmánková E, Komárková J (2000) Function of cyanobacterial mats in phosphorus-limited tropical wetlands. *Hydrobiol* 431:135–153
- Rejmánková E, Komárková J (2005) Response of cyanobacterial mats to nutrient and salinity changes. *Aquat Bot* 83(2):87–107
- Rejmánková E, Pope KO, Post R, Maltby E (1996) Herbaceous wetlands of the Yucatan peninsula: communities at extreme ends of environmental gradients. *Int Rev Gesamte Hydrobiol* 81:233–252
- Rejmánková E, Komárek J, Komárková J (2004) Cyanobacteria—a neglected component of biodiversity: patterns of species diversity in inland marshes of northern Belize (Central America). *Div Distrib* 10:189–199
- Richardson C, Vaithianathan P, Qualls RG (2008) Water quality, soil chemistry, and ecosystem response to P dosing. In: Richardson C et al (eds) *The Everglades experiments—lessons for ecosystem restoration ecological studies*, vol 201. Springer, New York, p 702
- Ruttenberg KC (1992) Development of a sequential extraction method for different forms of phosphorus in marine sediments. *Limnol Oceanogr* 37:1460–1482
- Sañudo-Wilhelmy SA, Tovar-Sanchez A, Fu FX et al (2004) The impact of surface-adsorbed phosphorus on phytoplankton Redfield stoichiometry. *Nature* 432:897–901
- Scinto LJ, Reddy KR (2003) Biotic and abiotic uptake of phosphorus by periphyton in a subtropical freshwater wetland. *Aquat Bot* 77:203–222
- Sharma K, Inglett PW, Reddy KR et al (2005) Microscopic examination of photoautotrophic and phosphatase-producing organisms in phosphorus-limited Everglades periphyton mats. *Limnol Oceanogr* 50:2057–2062
- Sirová D, Vrba J, Rejmánková E (2006) Extracellular enzyme activities in benthic cyanobacterial mats: comparison

- between nutrient-enriched and control sites in marshes of northern Belize Source. *Aquat Microbiol Ecol* 44: 11–20
- Stal LJ (1995) Physiological ecology of cyanobacteria in microbial mats and other communities. *New Phytol* 131:1–32
- Stal LJ, Caumette P (Eds) (1994) microbial mats: structure, development and environmental significance. NATO-ASI Series. Springer, New York
- Sutherland IW (2001a) The biofilm matrix—an immobilized but dynamic microbial environment. *Trends Microbiol* 9:222–227
- Sutherland IW (2001b) Biofilm exopolysaccharides: a strong and sticky framework. *Microbiology* 147:3–9
- Vadstein O (2000) Heterotrophic, planktonic bacteria and cycling of phosphorus. Phosphorus requirements, competitive ability, and food web interactions. *Adv Microb Ecol* 16:115–167
- Watanabe K, Imase M, Sasaki K et al (2006) Composition of the sheath produced by the green alga *Chlorella sorokiniana*. *Lett Appl Microbiol* 42:538–543